Volume 21, No 3 | International Journal of Radiation Research, July 2023

Assessment of image quality of two cone-beam computed tomography of the Varian Linear accelerators: Comparison with spiral CT simulator

H. Ragab[1,2*], D.M. Abdelaziz[2,3], M.M. Khalil[4], M.N. Yasein Elbakry[4]

[1]*Department of Radiation Oncology, Warith International Cancer Institute (WICI), University of Warith Al. Anbiyaa, Karbala, Iraq*
[2]*Department of Radiation Oncology, Baheya hospital for early detection and treatment of breast cancer, Giza, Egypt*
[3]*Department of Radiation Oncology, National Cancer Institute (NCI), Cairo University, Cairo, Egypt*
[4]*Department of Physics, Faculty of Science, Helwan University, Cairo, Egypt*

► ***Original article***

Corresponding author:
Hossam Ragab, MSc. & Ph.D.,
E-mail:
Hossam.Ragab1992@Outlook.sa

Received: August 2022
Final revised: December 2022
Accepted: February 2023

Int. J. Radiat. Res., July 2023; 21(3): 491-497

DOI: 10.52547/ijrr.21.3.19

Keywords: *Cone-beam computed tomography, image quality, TB-CBCT, iX-CBCT.*

ABSTRACT

Background: To assess and compare image quality characteristics of x-ray computed tomography (CT) and cone beam (CBCT) imaging systems of the Varian linear accelerator. ***Materials and Methods:*** The CatPhan®504, was examined on the CT simulator (SOMATOM Definition AS, VA48A) and two CBCTs (TrueBeam™ and Clinac® iX linear accelerators) attached to Varian linear accelerator. Image quality parameters including pixel value stability, spatial linearity, pixel size verification, uniformity, noise, spatial resolution, low contrast resolution, and contrast-to-noise ratio (CNR) were assessed using different scanning protocols. ***Results:*** The mean pixel values of regions of interest were stable for CT, TB, and iX-CBCT imaging. Noise on CT was slightly lower and was seen to decrease with increasing mAs, while CNR increased with CT mAs and two CBCTs. For all schemes, the Modulation Transfer Function (MTF) of the reconstructed image was limited by the pixel size. Low contrast targets for TB-CBCT were visible, with up to 6 and 2 targets for 1% and 0.5% for contrast, respectively. However, up to 4 targets of 1% contrast on iX-CBCT images are visible for the low-contrast objectives. Also, up to 8, 4, and 1 targets of 1%, 0.5%, and 0.3% contrast were visible for the low-contrast targets on CT images. ***Conclusions:*** CT and CBCT image quality parameters have been quantified and compared for clinical protocols in different mAs conditions. Selecting the right protocol will boost contrast, based on image quality criteria. The mAs can be decreased to minimize patient dosage.

INTRODUCTION

Cone-beam computed tomography (CBCT) mounted on a linear accelerator (LINAC) in radiotherapy departments increased the probability of routine imaging of the anatomy of the patient in the treatment position [1]. Comparing the anatomy in three dimensions (3D) with the planning computed tomography (CT) allows prompt correction of the positioning deviations before delivery of the treatment dose [2,3]. The major objectives of Image-Guided radiotherapy (IGRT) are to optimize treatment margins reduction, allow the use of sharp dose gradients common to intensity-modulated radiation therapy (IMRT), volumetric modulated arc therapy (VMAT), and interactively adapt to changes in the tumor during treatment [4]. Latest CBCT acquisition modes aim (a) to reduce the dose to a minimum, (b) to save the patient from excessive imaging dose, and (c) obtain enough bone contrast and soft tissue to perform regular system corrections. However, the reduced dosage can lead to limitations in the usability of the image sets acquired as the image quality and accuracy of the Hounsfield units (HU) decreases proportionally [5]. This problem is exacerbated by the essential problem that the large cone geometry causes more artifacts and scatter than the fan beam CT [6].

To resolve the specific output of each CBCT system, a quality assurance (QA) program was developed for the image quality of CBCT guidance [7]. This QA is a tool way to solve problems HU's homogeneity values and the uniformity and spatial resolution of multiple CBCT systems, and a tolerance limit for each parameter. Previous papers analyzed image quality aspects such as spatial resolution and CBCT noise based on the QA program. In these papers, the parameters of image quality were compared for different methods of reconstruction and different tube current settings [6,8]. Several studies have measured the efficiency of the CBCT image when affected by noise and resolution [9–14]. In CBCT, apart from the geometry and features of the scanner (tube current, tube voltage, mAs, and

[Downloaded from ijrr.com on 2026-11-22]

[DOI: 10.61186/ijrr.21.3.491]

focal spot size), the reconstruction filters often affect image quality with greater effects on resolution and noise than image uniformity [15].

This study uses the Varian TrueBeam™ and Varian Clinac® iX-CBCT images of the CatPhan®504 phantom. Image quality parameters of CNR, HU uniformity, pixel stability, and spatial resolution were assessed for full-fan and half-fan acquisition modes of CBCT. This study attempted to assess the imaging capabilities of two CBCT systems for IGRT implementation. The objective was to compare and provide an unbiased review of two commonly used CBCT systems.

MATERIALS AND METHODS

Catphan phantom setup

The Catphan®504 phantom (The Phantom Laboratory, New York, USA) is a cylindrical phantom build of multiple modules that can be used to measure different indices of image quality. The phantom is 20 cm in diameter, and 20 cm in length. The Catphan modules CTP 404, CTP 486, CTP 528, and CTP 515 were used for this study. For pixel value stability and pixel size verification, a CTP 404 package containing inserts of different densities was used; which includes air, acrylic, polystyrene, low-density polyethylene, teflon, and delrin with densities varying from 0-2.16 g/cm^3. CTP 486 has a standard 150 mm diameter water equivalent disk for determining HU uniformity. A spatial resolution of up to 21 lp/cm was assessed using CTP 528. Low contrast resolution was evaluated with CTP515 module [16].

Imaging devices and parameters of acquisitions

All scans included in this study were acquired using a helical CT simulator (Siemens, SOMATOM Definition AS, VA48A, Germany) and CBCT integrated with Varian TrueBeam™ and Varian Clinac® iX (Varian Medical Systems, Palo Alto, CA, USA) at 90° with respect to the treatment beam. In this study, the two CBCT models will be called TB and iX respectively (table 1). The 2D projection data of the Catphan®504 phantom was acquired three times for both full-fan and half-fan modes of iX-CBCT and acquired four times for full-fan and twice times for half-fan modes of TB-CBCT.

Pixel Value Stability

The CatPhan's reconstructed CTP 404 module slice was used to determine the stability of the pixel value for each of the inserts (figure 1). The seven different inserts were computed using means and standard deviation. Ideally, the mean value measured for the area of interest is representative of HU values (equation 1), and the SD in that area reflects noise (σ) [17]. Where μ_x is the linear attenuation coefficient of the material in question and μ_{water} and μ_{air} are the linear attenuation coefficients of water and air, respectively.

$$HU = 1000 * {\mu_x - \mu_{water}}/{\mu_{water} - \mu_{air}} \quad (1)$$

Spatial linearity and Pixel Size Verification

Verification of the pixel size of the image was carried out to ensure that the pixel size coincides with the nominal value. A rectangular ROI was used to calculate the number of pixels in the pin-to-pin distance, using the distance measurements from the spatial linearity calculation (figure 2). The pixel size was calculated using the equation 2 by knowing the distance between two pins and the number of pixels in that distance [16].

$$Pixel\ size = {distance\ to\ pin\ (mm)}/{\text{Number of pixels in that distance}} \quad (2)$$

Uniformity

The CTP 486 module of the Catphan containing a homogeneous material was used to quantify uniformity of the image. On the same slice of the Catphan image, rectangular ROIs were selected at the center and four peripheral regions figure 3. To evaluate the image uniformity the mean HU values of each ROI were calculated [17].

The difference between the pixel values from the peripheral region to the center of an image slice determines the uniformity of the image. The uniformity of the image was evaluated using the Uniformity Index (UI), as defined in equation 3.

$$UI = {(HU_{periphery} - HU_{center})}/{HU_{center}} \times 100 \quad (3)$$

Where HU periphery is the average HU value of all the four peripheral ROIs and HU center is the average HU value from the central ROI.

Noise

The standard deviation of pixel intensities over a region of interest (ROI) is indicative of the image noise. We used ROIs of 3mm × 3mm for evaluating noise as shown in figure 3. We didn't use larger ROIs to evaluate noise because of the result may be affected by artifacts in the image and the fact that it can lead to an increased standard deviation (SD) with ROI size [18].

Spatial resolution

The spatial resolution was measured using the CTP 528 module, containing 1 to 21 lp/cm (figure 4). The Modulation Transfer Function (MTF) that is a function of the spatial resolution of the imaging system has been evaluated. In this study, the MTF was evaluated based on the density change through each line pair pattern using the equation 4 [19].

$$MTF = {\pi/\sqrt{2} * \sqrt{M^2 - N^2}}/{|HU_{mean1} - HU_{mean2}|} \quad (4)$$

[Downloaded from ijrr.com on 2026-11-22]

[DOI: 10.61186/ijrr.21.3.491]

Where M is the noise within the line pair patterns, N is the noise within a uniform image area and HU_{mean1} and HU_{mean2} are the mean pixel values within uniform regions of different thickness or densities.

Low contrast resolution

The low contrast module CTP515 includes multiple objectives used to test the low contrast resolution efficiency of the imaging systems. Low contrast resolution refers to the ability of a machine to differentiate between objects with identical attenuation coefficients for x-rays. The CTP 515 module is composed of supra-slice and sub-slice targets as shown in figure 5. The supra-slice targets are three levels of contrast: 0.3%, 0.5%, and 0.1%. Each contrast level has nine supra-slice targets with diameters 2, 3, 4, 5, 6, 7, 8, 9, and 15 mm. additionally, there are three sub-slice target areas in the middle of the phantom, each with a contrast level of 1.0 %. Each area includes four targets with diameters ranging between 9 mm and 3 mm. The low contrast performance assessment was performed through visual analysis. The target areas of the supra-slice and sub-slice were assessed independently of one another. Supra-slice contrast was measured by the total number of visible targets at each contrast level and the cumulative amount was recorded [20].

Contrast-to-noise ratio (CNR)

CNR is defined as the difference between the average HU values in the insert and background, divided by (σ) Which is the standard deviation of the pixel values in a region of interest in the background [18]. The CNR of the insert was calculated using equation 5.

$$CNR = 2 \times {|HU_{insert} - HU_{background}|}/{(\sigma_{insert} + \sigma_{background})} \quad (5)$$

Statistical analysis

The Statistical Package for Social Sciences (SPSS Statistics) version 26.0 (IBM Corp., Armonk, USA) was used for statistical analysis.

Table 1. List of routine patient imaging protocols for TB, iX-CBCT, and CT simulator.

	Parameters	Head	Spotlight	Image Gently	Pelvis	Pelvis obese	Thorax
TB-CBCT	Fan Type	Full	Full	Full	Half	Half	Half
	Trajectory	Half	Half	Half	Full	Full	Full
	X Ray Tube Current, mA	20	100	13	80	99	20
	X Ray Tube Voltage, KV	100	125	80	125	140	125
	Exposure, mAs	150	750	100	1080	1687.5	270
	Exposure Time, s	7.515	7.5	7.5	13.41	17.005	13.425
	Focal Spot, mm	1	1	1	1	1	1
	Slice Thickness, mm	2	2	2	2	2	2
	Resolution(X*Y), mm	0.511*0.511	0.511*0.511	0.511*0.511	0.908*0.908	0.908*0.908	0.908*0.908
	Projections	500	500	500	900	900	900
	Matrix size	512	512	512	512	512	512
	CTDI vol, mGy	3.17	12.3	0.94	15.98	36.79	4
	Parameters	Standard Dose Head	Low Dose Head	High Quality Head	Pelvis Spot Light	Pelvis	Low Dose Thorax
iX-CBCT	Fan Type	Full	Full	Full	Full	Half	Half
	Trajectory	Half	Half	Half	Half	Full	Full
	X Ray Tube Current, mA	20	10	80	80	80	20
	X Ray Tube Voltage, KV	100	100	100	125	125	110
	Exposure, mAs	145	72	720	720	680	262
	Exposure Time, s	7.7	7.56	9.65	9.65	9.048	13.9
	Focal Spot, mm	0.1	0.1	0.1	0.1	0.1	0.1
	Slice Thickness, mm	2.5	2.5	2.5	2.5	2.5	2.5
	Resolution(X*Y), mm	0.651*0.651	0.651*0.651	0.651*0.651	0.651*0.651	1.172*1.172	1.172*1.172
	Projections	360	360	360	360	655	655
	Matrix size	384	384	384	384	384	384
	CTDI vol, mGy	3.9	2	19.4	14.4	17.7	4.7
	Parameters	Head	Thorax	Abdomen	Pelvis	Head& Neck Shoulder	
CT	Eff.mAs	410	140	250	270	200	
	KV	120	120	120	120	120	
	Scan time, s	13.14	14.52	19.13	14.71	11.44	
	Rotation time, s	1	1	1	1	1	
	slice, mm	3	4	4	4	4	
	Range, cm	16	32	32	32	32	
	Pitch	0.55	1.2	0.6	0.8	0.8	
	FOV	500	500	500	500	500	
	Collimation (X*Y), mm	16*1.2	16*1.2	16*1.2	16*1.2	16*1.2	
	Focal Spot, mm	1.2	1.2	1.2	1.2	1.2	
	Resolution(X*Y), mm	0.977*0.977	0.977*0.977	0.977*0.977	0.977*0.977	0.977*0.977	
	Matrix size	512	512	512	512	512	
	CTDI vol, mGy	68.57	11.33	20.23	21.89	16.22	

[Downloaded from ijrr.com on 2026-11-22]

[DOI: 10.61186/ijrr.21.3.491]

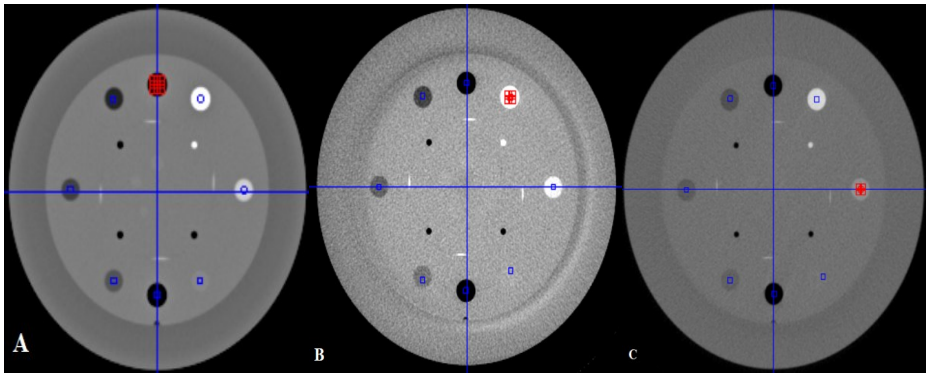
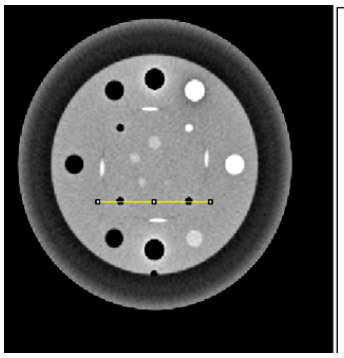


Figure 1. Image of CTP 404 module of Catphan with seven different inserts for **(a)** CT simulator **(b)** iX-CBCT **(c)** TB-CBCT at X Ray Tube Voltage = 100 kV and X Ray Tube Current = 80 mA.



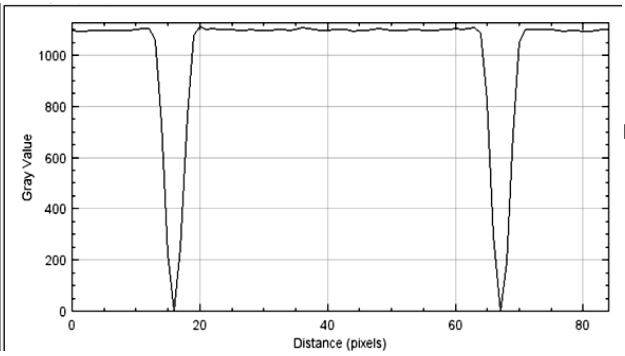


Figure 2. Image of CTP404 Module used to measure the pixel size by knowing the distance (50mm) between two pins and the number of pixels in that distance.

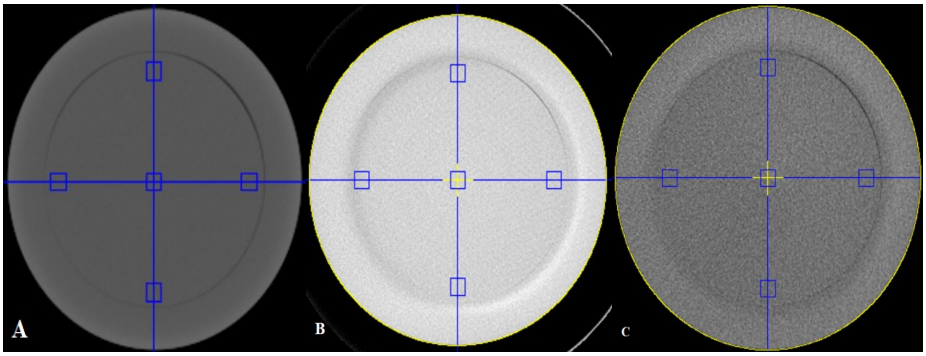


Figure 3. An axial slice view of the CTP 486 module of Catphan with ROIs drawn on **(a)** CT simulator **(b)** iX -CBCT **(c)** TB-CBCT at X-ray tube voltage = 100 kV and X-ray tube current = 80 mA.

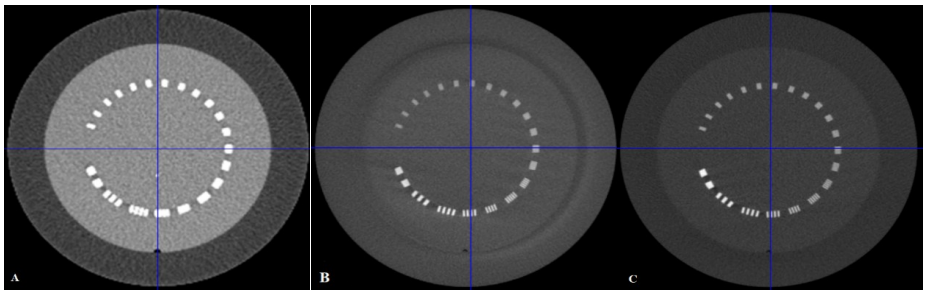


Figure 4. An axial slice view of the CTP528 Module was used to evaluate the high contrast spatial resolution on **(a)** CT scanning, **(b)** iX-CBCT scanning, and **(c)** TB-CBCT scanning.

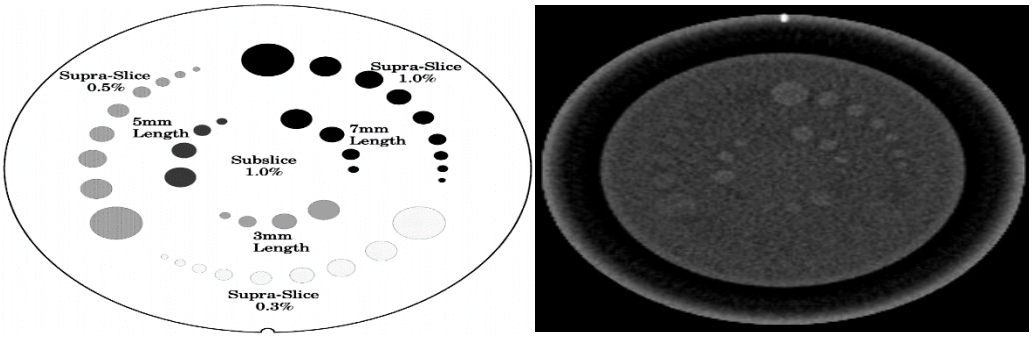


Figure 5. The CTP 515 module for low contrast resolution test with supra-slice and sub-slice contrast targets.

[Downloaded from ijrr.com on 2026-11-22]

[DOI: 10.61186/ijrr.21.3.491]

RESULTS

Pixel Value Stability

The calculated mean pixel values for 3 mm diameter circular ROIs in different Catphan module inserts, CTP 404, were recorded for full-fan and half-fan modes. Insert pixel values were stable when mAs varied with imaging system except for one or two values. The mean pixel values in the ROIs for the different protocols of the various CTP 404 module inserts were -1000±9, -200±15, -100±21, -35±32, 120±45, 340±122, and 990±384 HU for TB-CBCT scanning protocols whiles values of -1000±30, -200±126, -100±130, -35±120, 120±104, 340±89, and 990±181 HU for iX-CBCT scanning protocols. For CT scanning protocols -1000±16, -200±18, -100±15, -35±13, 120±12, 340±18, and 990±39 HU in air, PMP, LDPE, polystyrene, acrylic, delrin, and teflon, respectively. It was seen that with an increase in HU values, i.e., with an increase in relative densities, the difference in HU between the measured and expected values increases. The highest density insert, Teflon, recorded a large HU difference of 384 HU on TB-CBCT and 181 HU on iX-CBCT when compared to the expected values [21].

Spatial linearity and pixel size verification

The CBCT imaging protocols used two-pixel sizes as shown in table 1. The pin distances measured for all images (CT, TB, and iX-CBCT) are within a nominal distance of 2 %. All images are within 1%; except for the low dose thorax protocol of iX-CBCT which is 1.56%. Most of the distances measured are near the nominal value, and little variation is found. The greatest difference between the measured and nominal pixel size was 0.015 mm, giving the head and neck and pelvis protocols an error of 1.54% for CT. The smallest error in the pelvis, pelvis obese, and thorax protocols for TB-CBCT between the measured and nominal pixel size is 0.11 %.

Uniformity

Table 3 shows measurements of the UI on a reconstructed slice of Catphan using various mAs in CT simulator, TB, and iX-CBCT full- and half-fan modes. It was found that some of the HU values at the peripheral ROI were higher than those of the central ROI for both full-fan and half-fan modes likely due to 'cupping artifact' and the other HU values at the peripheral ROI were lower than those of the central ROI, due to 'capping artifact'.

The average values of the UI are 0.48, -1.16, 2.09, 0.047, and 0.25 for full fan and half fan on TB, iX-CBCT, and CT simulator, respectively.

Noise

For CT and CBCTTB, iX, the image noise was decreased as tube mAs has increased. As shown in table 3, the values of the noise for full fan and half fan on CBCTTB, iX and CT simulator. An overall reduction of the values of the noise with increasing mAs was also observed for CBCTTB, iX at half fan compared to a full fan.

Spatial resolution

MTF measurements using different protocols for full- and half-fan modes are shown in table 2. The number of line pairs determined by all protocols indicates limited variance in CT, TB, and iX-CBCT imaging for both full-fan and half-fan modes at 50 % MTF (~0.4 lp/mm for full-fan and ~0.3 lp/mm for half-fan).

Table 2. The MTF measurement with the frequencies corresponding to the MTF values of 0.5 and 0.1 for CT, TB, and iX-CBCT imaging protocols.

CT					
	Head	Head & Neck Shoulder	Pelvis	Thorax	Abdomen
$f_{0.5}$ (mm^{-1})	0.28	0.33	0.36	0.38	0.34
$f_{0.1}$ (mm^{-1})	0.49	0.49	0.58	0.64	0.69
TB-CBCT					
	Full Fan			Half Fan	
	Head	Spotlight	Image gently	Pelvis	Pelvis Obese	Thorax
$f_{0.5}$ (mm^{-1})	0.38	0.34	0.54	0.22	0.28	0.2
$f_{0.1}$ (mm^{-1})	0.71	0.61	0.87	0.44	0.46	0.44
iX-CBCT						
	Full Fan				Half Fan	
	Standard dose head	Low dose head	High-quality head	Pelvis spotlight	Pelvis	Low dose thorax
$f_{0.5}$ (mm^{-1})	0.44	0.37	0.44	0.47	0.34	0.32
$f_{0.1}$ (mm^{-1})	0.79	0.61	0.78	0.87	0.53	0.42

Low contrast resolution

With the increase in mAs, the visibility of the low contrast targets for CT, TB and iX-CBCT were improved. While low contrast targets on TB-CBCT were visible, up to 6 and 2 targets, respectively, of 1% and 0.5% contrast were visible for the highest mAs setting (i.e., 750 mAs) using the full-fan mode, and up to 6 of the targets were visible for half-fan mode at the 1687.5 mAs (Pelvis obese). However, the low-contrast targets are visible up to 4 targets at 1% contrast on iX-CBCT images for full-and half-fan mode. Also, the low-contrast targets on CT images were visible, up to 8, 4, and 1 targets, respectively, of 1%, 0.5%, and 0.3% contrast were visible in the mAs range from 140 to 410.

Contrast-to-noise ratio (CNR)

Table 3 shows the different CNR for each CT, TB, and iX-CBCT imaging protocols. In general, The CNR increases with increasing mAs for CT, TB, and iX-CBCT. That because noise decreases with increasing mAs, and pixel values with different mAs are relatively constant. The head, pelvis obese, and pelvis spotlight protocols have the greatest CNR with values of 3.91, 1.63, and 1.21, respectively on CT, TB,

[Downloaded from ijrr.com on 2026-11-22]

[DOI: 10.61186/ijrr.21.3.491]

and iX-CBCT. The lowest CNR on CT, TB, and iX-CBCT images were thorax, image gently, and low dose head protocols with values of 1.21, 0.26, and 0.25, respectively.

Table 3. Measurement values of the uniformity index (UI), noise (SD), and contrast-to-noise ratio (CNR) for various scanning protocols for CT, TB and iX-CBCT.

Protocols			kV	mAs	UI	SD	CNR
CT simulator	Head		120	410	-0.02	0.35	3.91
	Head& Neck Shoulder		120	200	0.33	1.03	1.24
	Thorax		120	140	0.27	1.06	1.21
	Abdomen		120	250	0.39	0.9	1.59
	Pelvis		120	270	0.27	0.92	1.74
TB-CBCT	**Image Gently**	Full Fan	80	100	2.12	5.53	0.26
	Head	Full Fan	100	150	2.03	2.85	0.4
	Spotlight	Full Fan	125	750	-2.7	0.79	0.13
	Thorax	Half Fan	125	270	-2.24	1.25	0.84
	Pelvis	Half Fan	125	1080	-0.62	1.01	1.44
	Pelvis obese	Half Fan	140	1687.5	-0.62	0.79	1.63
iX-CBCT	**Low Dose Head**	Full Fan	100	72	1.77	3.87	0.25
	Standard Dose Head	Full Fan	100	145	2.57	3.36	0.39
	High Quality Head	Full Fan	100	720	2.15	2.11	1.07
	Pelvis Spot Light	Full Fan	125	720	1.88	1.65	1.21
	Low Dose Thorax	Half Fan	110	262	0.47	0.97	0.82
	Pelvis	Half Fan	125	680	0.47	0.84	0.96

DISCUSSION

The overall aim of this work was to evaluate image quality of CT simulator (Siemens, SOMATOM Definition AS, VA48A, Germany) and two different cone-beam machines (TB and iX-CBCT) provided by the same manufacturer (Varian Medical Systems, Palo Alto, CA, USA) in terms of many performances and image quality parameter. The image quality parameters of the CT, TB, and iX-CBCT imaging systems were evaluated quantitatively to assess the optimum acquisition mode to be used for the volumetric imaging protocols. Catphan504 was a successful tool in quantifying and interpreting the results obtained from the three different systems. These tests included pixel value stability, spatial linearity, pixel size verification, uniformity, noise, spatial resolution, low contrast resolution, and CNR.

The current CBCT image quality evaluation typically focuses on various factors, as previously described in studies, including building a quality assurance framework for fully automated and time-efficient performance evaluation [22], evaluating imaging characteristics just within the axial slice [23,24], and looking at the CBCT device's long-term stability [7,25].

The pixel value stability differed between the CT and CBCT systems. There were large variations in the HU values between the CT and CBCT systems, there were also fairly significant HU fluctuations between the imaging protocols used by each system. It was seen that although the two CBCTs showed inconsistent HU accuracy, the TB-CBCT images demonstrated a better estimation of the HU revealed by the CT data. This shows how HU values can differ significantly due to changes in imaging parameters (object size, kV, mAs, pitch, and fan type).

The calculated MTF of the CT and CBCT images for each protocol was relatively similar, although the resolution calculated in the selected CT images was lower than that of the CBCT. MTF depends on a number of variables, which is the reason behind the difficulty to establish the direct contrast between CBCT and CT images. The imaging protocol can use several techniques that eventually affect their spatial resolution capabilities. The MTF of the imaging system can differ depending on slice thickness, pixel size, focal spot size, the field of view, image matrix, and detector size. But it was the pixel size that was critical to the MTF calculation because we did the calculated MTF at the axial slice view of the CTP528. The TB and iX-CBCT images of the head, spotlight, image gently, standard dose head, low dose head, high-quality head, and pelvis spotlight use smaller pixel sizes than the CT images for the same anatomy, so higher results appeared at 50% and 10% MTF. Thus, the CBCT images have a marginally better resolution than the oncology CT images by using the standard imaging protocols on each system.

Since the average noise and average uniformity index were higher in CBCT than in CT images. It was observed that with the increase in mAs, the noise decreased and the maximum average noise was reported on the TB-CBCT when the full fan was used. The large differences in image density between the maximum and minimum HU values resulted in a 'capping artifact' on TB-CBCT (pelvis, pelvis obese, thorax, and spotlight) and a 'cupping artifact' on TB and iX-CBCT. In contrast, the CT images showed no artifacts, resulting in lower capping artifacts. Where the highest capping artifact value was -2.7 on TB-CBCT for spotlight protocol and the highest cupping artifact value was 2.57 on iX-CBCT for standard dose head.

In the low contrast resolution test, the most important difference was found between the CT and CBCT images. The CBCT system inability to detect low contrast targets significantly restricts its capability for diagnostic scanning [26]. It is possibly due to an increase in image noise in the CBCT images. The CBCT beam is considerably larger than traditional fan-beam geometry, allowing more scatter into the system. The composition and configuration of the detector may also lead to a greater amount of noise. The CBCT uses a flat panel detector with a large imaging area that allows for more scattered radiation to be detected than CT. The difference between the CT and CBCT image techniques in mAs is a major parameter in image quality and noise levels. By using a higher mAs, the number of photons absorbed in the detector will increase reducing

[Downloaded from ijrr.com on 2026-11-22]

[DOI: 10.61186/ijrr.21.3.491]

statistical counting uncertainty.

In our study we also calculated CNR of the different imaging protocols for TB and iX-CBCT have a much lower CNR than the CT images. In table 3, this data also reflects the results of the low contrast resolution analysis in which only a few targets are visible with low CNR images. We also observe that the highest CNR value in each system for the mAs and kV is highest, followed by increased $CTDI_{vol}$ exposure of the patient. The relationships in this work are intended to be an analysis of the image quality versus different protocols for various systems. The physicists can use it for the creation, when deciding clinical scanning protocols for their respective needs, of a good dose-to-image-quality compromise in making responsible clinical decisions.

CONCLUSIONS

On two CBCT widely used and commercially available models we analyzed the effects of various protocols on image quality and compared them with CT simulator. Various image quality parameters were assessed to evaluate image quality using an extensive series of clinically relevant imaging protocols using CatPhan504. Using different protocols, the image quality of CBCT's full-fan and half-fan acquisition modes was evaluated. The choice of different protocols could improve the image quality, making it easier for radiation oncologists to contour structures and image registrations. The choice of the suitable protocol will improve contrast, depending on the requirements of image quality.

ACKNOWLEDGEMENT

The authors are thankful to radiotherapy staff of Baheya Hospital (Giza, Egypt) for their type assist on this study.

***Funding*:** This research did not receive any specific grant from funding agencies in the public, commercials, or not for profit sectors.

***Conflict of interest*:** The authors of this manuscript declare no relationships with any companies whose products or services may be related to the subject matter of this article.

***Ethical statement*:** This retrospective study was approved by the medical ethics committee of Baheya hospital.

***Author contribution*:** H. Ragab designed the study, performed the statistical analysis, and drafted the manuscript. review and editing; D.M. Abdelaziz and M.M. Khalil. Supervision D.M. Abdelaziz, M.M. Khalil and M.N. Yasein Elbakry. All authors read and approved the final manuscript.

REFERENCES

1. Jaffray DA, Siewerdsen JH, Wong JW, Martinez AA (2002) Flat-panel cone-beam computed tomography for image-guided radiation therapy. *Int J Radiat Oncol, **53**(5): 1337-49*.
2. Elstrøm U V, Wysocka BA, Muren LP, *et al.* (2010) Cone-beam CT and deformable image registration as a method for studying dosimetric consequences of anatomic changes in adaptive IMRT of head and neck cancer. *Acta Oncol (Madr), **49**(7): 1101-8*.
3. Dawson LA and Jaffray DA (2007) Advances in image-guided radiation therapy. *J Clin Oncol, **25**(8): 938-46*.
4. Verellen D, Ridder M De, Storme GA (2008) Short history of image -guided radiotherapy. *Radiother Oncol, **86**(1): 4-13*.
5. Kim S, Yoo S, Yin F-F, *et al.* (2010) Kilovoltage cone-beam CT: Comparative dose and image quality evaluations in partial and full -angle scan protocols. *Med Phys, **37**(7Part1): 3648-59*.
6. Elstrøm U V, Muren LP, Petersen JBB, Grau C (2011) Evaluation of image quality for different kV cone-beam CT acquisition and reconstruction methods in the head and neck region. *Acta Oncol (Madr), **50**(6): 908-17*.
7. Bissonnette J-P, Moseley DJ, Jaffray DA (2008) A quality assurance program for image quality of cone-beam CT guidance in radiation therapy. [Internet] *Med Phys, **35**(5):1807-15*.
8. Kamath S, Song W, Chvetsov A, Li J, *et al.* (2011) An image quality comparison study between XVI and OBI CBCT systems. *Med Phys, **35**(6): 2648*.
9. Miura H, Ozawa S, Hayata M, *et al.* (2017) Evaluation of cone-beam computed tomography image quality assurance for Vero4DRT system. [Internet] *Reports Pract Oncol Radiother, **22**(3): 258-63*.
10. Zhang J, Bao ZR, Huang XT, *et al.* (2019) Methods to evaluate the performance of kilovoltage cone-beam computed tomography in the three-dimensional reconstruction space. *Int J Radiat Res, **17**(2):189-202*.
11. Chen L, Shaw CC, Mustafa C, *et al.* (2008) Spatial resolution properties in cone beam CT: A simulation study. *Med Phys, **35**(2): 724-34*.
12. Endo M, Tsunoo T, Nakamori N, Yoshida K (2001) Effect of scattered radiation on image noise in cone beam CT. *Med Phys, **28**(4): 469–74*.
13. Jaffray DA and Siewerdsen JH (2000) Cone-beam computed tomography with a flat-panel imager: Initial performance characterization. *Med Phys, **27**(6): 1311-23*.
14. Yang K, Kwan ALC, Huang S-Y, *et al.* (2008) Noise power properties of a cone-beam CT system for breast cancer detection. *Med Phys, **35**(12): 5317-27*.
15. Shepherd J (2014) Applications of linac-mounted kilovoltage Cone -beam Computed Tomography in modern radiation therapy: A review. *Polish J Radiol, **79**: 181-93*.
16. The Phantom Laboratory (2013) Catphan ® 504 Manual CTP504. 2013.
17. EFOMP-ESTRO-IAEA (2019) Quality control in cone-beam computed tomography (CBCT) EFOMP-ESTRO-IAEA protocol. 2019.
18. IAEA (2012) Quality Assurance Programme for Computed Tomography: Diagnostic and Therapy Applications, Human Health Series No. 19. Vienna; 2012.
19. Droege RT and Morin RL (1982) A practical method to measure the MTF of CT scanners. *Med Phys, **9**(5): 758-60*.
20. Gulliksrud K, Stokke C, Trægde Martinsen AC (2014) How to measure CT image quality: Variations in CT-numbers, uniformity and low contrast resolution for a CT quality assurance phantom. *Phys Medica, **30**(4): 521-6*.
21. Roa AMA, Andersen HK, Martinsen ACT (2015) CT image quality over time: comparison of image quality for six different CT scanners over a six-year period. *J Appl Clin Med Phys,**16**(2): 350-65*.
22. Steiding C, Kolditz D, Kalender WA (2014) A quality assurance framework for the fully automated and objective evaluation of image quality in cone-beam computed tomography. [Internet] *Med Phys, **41**(3): 031901*.
23. Cheng HCY, Wu VWC, Liu ESF, Kwong DLW (2011) Evaluation of radiation dose and image quality for the Varian cone beam computed tomography system. *Int J Radiat Oncol Biol Phys, **80**(1): 291 -300*.
24. Stock M, Pasler M, Birkfellner W, *et al.* (2009) Image quality and stability of image-guided radiotherapy (IGRT) devices: A comparative study. [Internet] *Radiother Oncol, **93**(1): 1-7*.
25. Sumida I, Yamaguchi H, Kizaki H, *et al.* (2014) Evaluation of imaging performance of megavoltage cone-beam CT over an extended period. *J Radiat Res, **55**(1): 191-9*.
26. Lechuga L, Weidlich G A. (September 12, 2016) Cone Beam CT vs. Fan Beam CT: A Comparison of Image Quality and Dose Delivered Between Two Differing CT Imaging Modalities. *Cureus **8(9):** e778. DOI 10.7759/cureus.778*

[Downloaded from ijrr.com on 2026-11-22]

[DOI: 10.61186/ijrr.21.3.491]

[DOI: 10.61186/ijrr.21.3.491] [Downloaded from ijrr.com on 2026-11-22]